25th ABCM International Congress of Mechanical Engineering
October 20-25, 2019, Uberlândia, MG, Brazil

# COB-2019-XXXX
# THERMAL PERFORMANCE OF SILVER WATER/EG NANOFLUIDS IN RECTANGULAR CROSS SECTION MICROCHANNELS HEAT SINK

**Luz Elena Peñaranda Chenche**
**Ítalo Franco Guilherme**
**Enio Pedone Bandarra Filho**
Federal University of Uberlandia, Av. João Naves de Avila, 2121, Uberlândia (MG)-Brazil
e-mails: ing.elenap@gmail.com, italoengmec95@gmail.com, bandarra@ufu.br

**Carolina Naveira Cotta**
Federal University of Rio de Janeiro, COPPE, Av. Horácio Macedo, 2.030, Rio de Janeiro (RJ) - Brazil
e-mails: carolina@mecanica.ufrj.br

***Abstract.*** *In this paper the thermal performance of silver nanofluid used as a coolant into a rectangular cross section microchannel heat sink is analyzed by evaluating the convective heat transfer coefficient and the thermal resistance of the fluids. For the synthetizing process of the nanofluid it was used silver nanoparticles powder with diameter of 80 nm. The based fluid is composed by 50% of distilled water and 50% of ethylene glycol. The solution is diluted using the ultrasonic disrupt method, resulting in a nanofluid with volume concentrations of 0.0005%, 0.001% and 0.005%. The thermophysical properties such as thermal conductivity and viscosity of the samples were experimentally measured. Then, the nanofluids were test in an experimental facility under different mass flow, heat flux and inlet fluid temperature conditions. From the experimental results, there was not observed significate differences between the viscosity of nanofluids and the base fluid. However, it was obtained enhancements in the thermal conductivity related to the volume concentration of nanoparticle. A maximum enhancement of in the convective heat transfer coefficient of the heatsink 44.8%, and in the thermal resistance of 21.7% was observed for the highest concentration nanofluid.*

***Keywords:*** *Nanofluids, Microchannel heat sink, heat transfer, pressure drop*

## 1. INTRODUCTION

Cooling is one of the most important challenges facing numerous industrial sectors. In this sense, Microchannel heat sink were first time introduced by Tuckerman and Pease (1981) as cooling solutions in electronic systems to dissipate high heat fluxes in small areas, and have since become one of the most important methods of heat removal in many engineering applications such as high power electronics for the automotive industry, electronics cooling, solar and nuclear components, pumps, biomedical and biochemical analysis instruments (Anbumeenakshi; Thansekhar, 2017).

Microchannel heat sinks are compact devices, typically defined by their dimensions, from 10 to 200 μm, but up to 1 to 3 mm in some applications, such as single-phase liquid flow, boiling and condensation (Kandlikar, et al., 2013).. The basic design of microchannel heat exchangers consists of a series of rectangular cross section linear channels, as shown in Fig. 4, although according to Gilmore, Timchenko and Menictas (2018) there are a number of literatures claiming that straight microchannels may not be the better channel configuration to obtain a high thermal performance of heat sink. Hence, different methods to enhances the heat transfer processes in microchannels has been proposed, some of them includes complex cross section shapes as triangular, (Chu, Teng and Greif, 2008), circular, hexagonal, rhombus (Alfaryjat, Mohammed, et al., 2014), trapezoidal, concave or convex (Tran et al., 2017) , or incorporates porous medium (Dehghan, Valipour and Saedodin, 2016) to the channel section among others. However, this kind of solution involves a high fabrication cost of the microchannels heat sink and despite the considerable amount of research and development focusing on heat transfer improvements by change the geometry of the cooling device, major development in cooling capability are still insufficient because conventional heat transfer fluids possess non optimal heat transfer properties. Consequently, the advent of nanotechnology that made possible to synthesize particles in nanometric scale (1-100 nm) and dispersing those in conventional cooling fluids, named by Choi, (1995) as nanofluids arise as a promising alternative to enhance the heat transfer capacity of the working fluids in thermal processes. The immediate consequences of add nanoparticles in cooling fluids are reflected in its thermophysical properties. There are several works focus in the study of the behavior of thermophysical properties of nanofluids, most of them report that increasing

of nanoparticle concentration in the fluid result in an increase of thermal conductivity, viscosity and specific mass while the specific heat decreases.

Among the different nanoparticles materials, silver stands out due to the high thermal performance reported in literature. Cárdenas Contreras et al. (2019) recently evaluated experimentally the thermohydraulic performance of silver (Ag) nanofluids, with a binary mixture of water and ethylene glycol (50:50 vol.%) as a base fluid, with nanoparticles concentrations of 0.01, 0.05 and 0.1 vol.%. The experiments were performed in an automotive radiator. Was reported an increase up to 4.4% in the heat transfer rate with the Ag nanofluid and, in the condition of 0.08 kg/s mass flow rate and 55-65 °C temperature range, the thermohydraulic performance reached a 2.5% average increase in relation to the base fluid. In different applications, other publications have also achieved positive results with silver nanoparticle in different base fluids. (Sarafraz et al., 2018) published an increase in heat transfer coefficient of 47% compare to the base fluid with 0.1% mass concentration of Ag/water nanofluid. A higher increment in heat transfer coefficient was achieved by Godson et al. (2012), with 0.9 vol.% of silver nanofluid, increasing 69% compare to the base fluid. (Pourhoseini et al., 2018) also worked with Ag/water nanofluid and detected that at some critical nanofluid concentration (2.5 mg/L), the rate of heat transfer reaches its maximum. The thermal conductivity of the nanofluid in such a state was 36.6% greater than that of pure water. Related to thermal conductivity property, Aberoumand et al. (2016) recently reported their experimental data of Ag/thermal oil (TO) nanofluids. They reported that different from the base fluid, the thermal conductivity of the nanofluids increases as the temperature increased. This increasing trend has been repeated for all the concentrations and was reported improvements in the thermal conductivity values of approximately 40%.

## 2. METHODOLOGY

Following is a description of the methodology implemented in this work, including the preparation of nanofluids, measurement of its thermophysical properties, the details of the experimental facility used to evaluate the heat transfer of nanofluids into microchannel heat sink in laminar flow, the geometric details of the microchannel heat sink and the data reduction. recommendations to authors

### 2.1 Nanofluids preparation

The synthesizing process of the fluids begins with the mixture of ethylene glycol and distilled water with a masa concentration of 50% of each one to complete a total volume of 1l. The required masses of base fluid (H2O + EG) and nanoparticles were measured with a precision balance. Then, the Ag nanoparticles with a diameter of 80 nm were dispersed in the base fluid by ultrasonic disrupt method using a Qsonica® sonicator model Q500 that have a working power of 500 W with a frequency of 20 kHz. The sonicator allows to configure working cycles in a period of time. This process was performed for 60 minutes. The volumetric concentration of the samples was 0.0005% for sample 1 (Ag_80_1), 0.001% for sample 2 (Ag_80_2) and 0.005% for sample 3 (Ag_80_3).


Figure 1. Qsonica® sonicator model Q500 and nanofluid

### 2.2 Measurement of thermopysical properties

The characterization of thermophysical properties of nanofluids is a process that was performed simultaneously with other stages of the work. Once the nanofluid samples were prepared, they were characterized to determine their thermophysical properties with the equipment that has the LEST-nano laboratory. Mainly, the specific mass, thermal conductivity and dynamic viscosity of all samples produced were measured and experimentally evaluated.

The specific mass and the dynamic viscosity of the nanofluids and base fluid samples were measurement with the Anton Paar viscometer (Stabinger ™ Model SVM ™ 3000) viscometer (Fig. 2a) that has an uncertainty of ±0.35%. The

physical principle for determining viscosity is based on the flow between parallel and infinite flat plates. The measurement range and uncertainties are presented in Table 1.

Thermal conductivity is measured by the thermal properties' analyzer Linseis THB1 (Transient Hot Bridge) with an uncertainty less than 2%. The THB method that is used to measure the thermal properties of materials, is an evolution of the transient hot wire (THW) method that follows the guideline of the standard (DIN EN 993-14, DIN EN 993-15). The THB method uses the probe to emits a constant heat flux over a period of time and simultaneously acquires the temperature values of the material or fluid. Therefore, the thermal conductivity is established as a function of the temperature-time relationship and the geometrical characteristics of the probe, under the hypothesis that the probe is a point heat source that is immersed in a homogeneous isotropic medium.

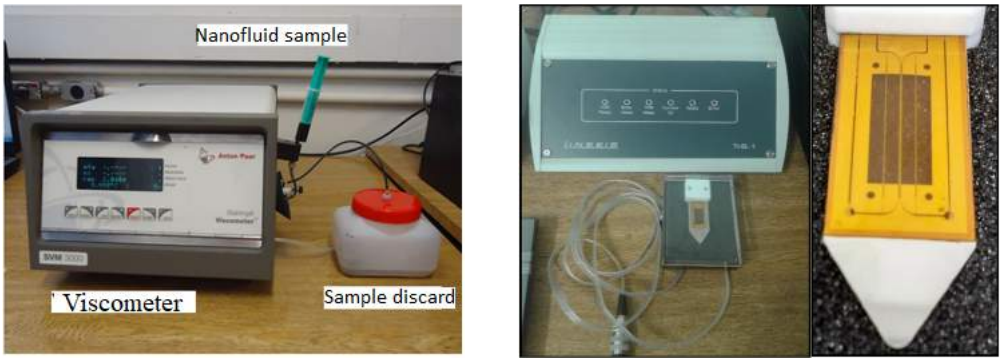


(a) (b)

Figure 2. (a) Anton Paar viscometer (Stabinger ™ Model SVM ™ 3000). (b) Linseis THN1 thermal properties' analyzer and probe.

The specific mass of the nanofluids is directly related to the volume fraction (Φ) of nanoparticles on the bas fluid. For this, Eq. (1) can be employed to calculate this property.

$$\rho_{nf} = (1-\phi)\,\rho_{bf} + \phi\,\rho_{np} \tag{1}$$

Although, for calculating the specific heat of nanofluids it was used a model proposed by O'Hanley et al.*[CITATION Har12 \n \t \l 1046 ]*. The model is based on the assumption of the thermal equilibrium between the particles and the surrounding fluid, which applying the first law of thermodynamics gives rise to the mathematical model in Eq. (2). This model was applied in the work of Wang et al.*[CITATION BuX10 \n \t \l 1046 ]* with satisfactory results.

$$c_{p,nf} = \frac{(1-\phi)\,(\rho c_p)_{bf} + \phi\,(\rho c_p)_{np}}{(1-\phi)\,\rho_{bf} + \phi\,\rho_{np}} \tag{2}$$

### 2.3 Experimental Facility

An experimental facility was built to test the micro channel heat sink under different heat conditions and to allow the evaluation of the thermal performance of the different fluids. As shown in the diagram in Fig. 3, the facility disposes of a controlled gear pump to maintain the fluid circulating at fixed flow rates. After the pump, it was placed a preheater to control the fluid temperature at the inlet of the microchannel heat sink. A turbine flowmeter, used to measure the volume flow rate of the fluid through the microchannel heat sink and two piezoelectric transmitters measure the pressure at the inlet and outlet of the microchannel heat exchanger. The pressure drop is redundant measure with a differential pressure transmitter. To achieve the boundary condition of constant heat flux it was used a cartridge resistor into a copper sheath and a controlled D.C power source. The power supplied by the D.C power source to the resistor was measured through two precision multimeters. To avoid heat loss by natural convection, the exposes surfaces of the microchannel heat sink were insulated using a layer of flexible elastomeric foam with a thickness of 5 mm in the lateral faces and 10 mm in the bottom face. Temperatures at the inlet and outlet flow in microchannel heat sink and in the contact interface between the heater ante the top surface of the microchannels were measured using Type "T" thermocouples. All the measured quantities were logged and recorded by a data acquisition system. The uncertainties of all the instruments used in the experimental facility are present in Tab. 1.

Table 1. Uncertainties of measurements instruments in the experimental facility.

| Instrument | Measurement range | Uncertainty |
|---|---|---|
| Thermocouples | -200 a 350 °C | ± 0.2° C |
| Pressure transmitters | 0-50 kPa | ±0,6 kPa |
| Pressure drop transmitter | 0-10 kPa | ± 2 % |
| Turbine flow transmitter | 0-100 ml/min | ± 0,3ml/min |
| Current Multimeter | 0-10 A | ± 3% |
| Voltage Multimeter | 0 -25 V | ± 3% |

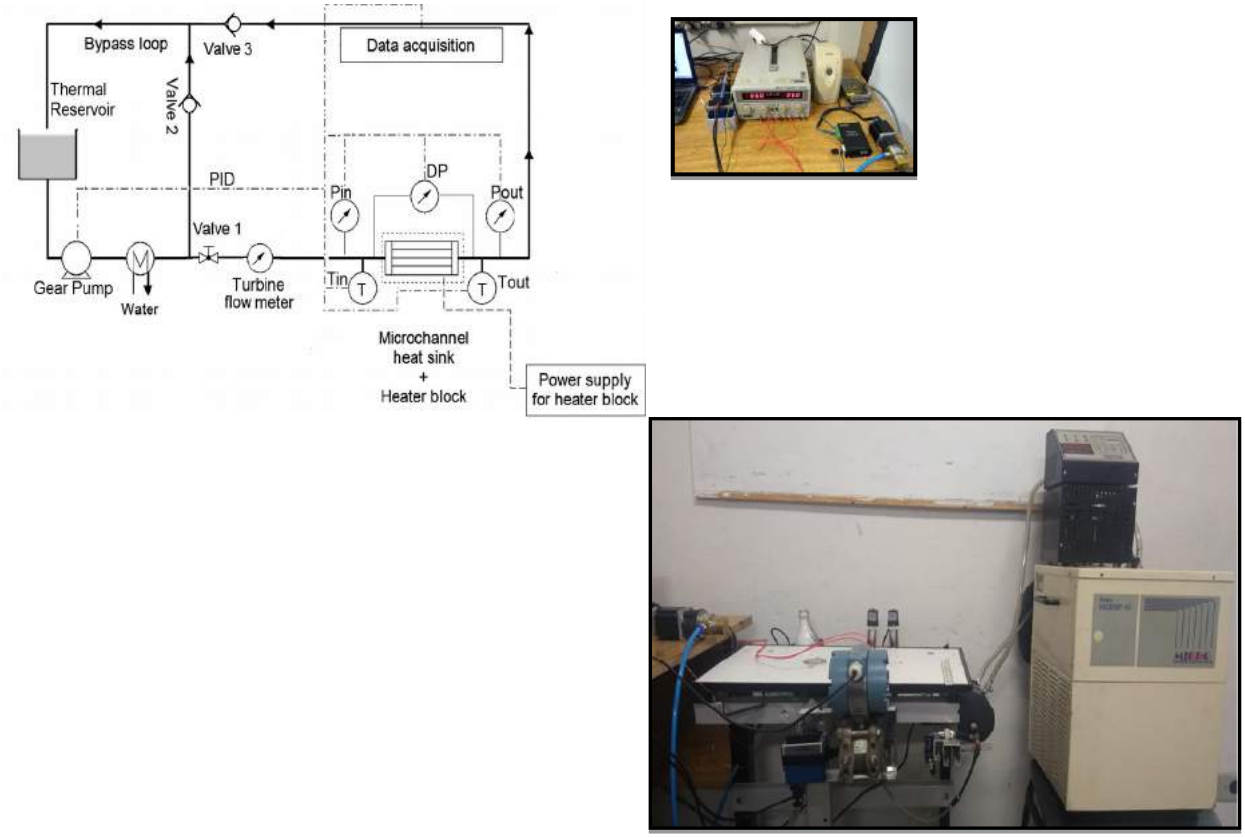


Figure 3. Experimental facility to evaluated heat transfer in microchannel heat sinks: (a) Schematic (b) Photography.

The microchannel heat sink used in this work was supplied by the Nano and Microfluidics and Microsystems Laboratory (LabMEMS) from UFRJ. The geometric structure of the microchannel heat sink is depicted schematically in Fig. 4 with the detailed dimensions summarized in Tab. 2. Twenty-four parallel rectangular microchannels machined into aluminum block to form the microchannel heat sink. Each microchannel have cross-sectional area of 400 μm in width (W) and 945 μm in height (H) with a total length (L) of 50 mm with. All the microchannels are equidistantly spaced with a fin width (t) of 160 μm. The microchannel heat sink block has an inlet and outlet pendulums at two ends of the microchannels to provide relative uniform flow distribution.

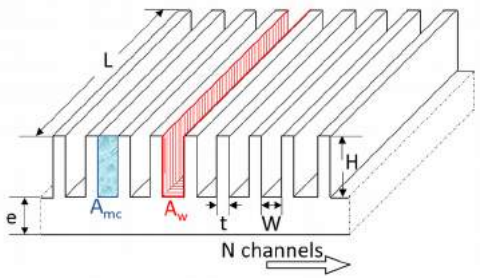


Figure 4. Microchannel heat sink.

Table 2. Main geometrical parameters of the microchannel heat sink.

| W (μm) | H (μm) | t (μm) | L (mm) | e (mm) | N |
|---|---|---|---|---|---|
| 400 | 945 | 160 | 400 | 2,05 | 24 |

The forced convection heat transfer experiments have been undertaken for the microchannel heat sink using the base fluid (H2O+EG) and the silver nanofluids synthetized (Ag_80_1,2,3) as the working fluid under the following operating conditions: the volume rate (v) from 15 to 60 ml/min, the inlet temperature Tin = 25– 35° C, and the heat flux ($Q_h$) in 5.2, 10.4 and 15.6 kW/m$^2$.

### 2.4 Data reduction

The steady-state heat transfer rate removed by the fluid flowing through the heat sink, $Q_c$ can be determined as follow:

$$Q_c = \rho \dot{v} c_p \left( T_{in} - T_{out} \right) \tag{3}$$

Where $Q_c$ is the removed heat, v is the volume rate, ρ is the specific mass of the fluid, $c_p$ is the specific heat of the fluid and $T_{out}$ and $T_{in}$ are the outlet and inlet fluid temperature, respectively.

Afterward, the convective heat transfer coefficient of the fluids for all cases was calculated based on the Newton's cooling law, described by equations Eq. (4).

$$h = \frac{Q_c}{A_w \cdot \mathrm{LMTD}} \tag{4}$$

where $A_w$ is the internal surface of the microchannel (Fig. 4) defined by Eq. (5) and LMTD is the logarithmic mean temperature difference between the wall temperature ($T_w$) of the microchannel heat sink and the fluid temperatures, presented in the Eq. (6).

$$A_w = \left( 2H + W \right) L \tag{5}$$

$$LMTD = \frac{\left( T_w - T_{in} \right) - \left( T_w - T_{out} \right)}{\ln \left( \frac{T_w - T_{in}}{T_w - T_{out}} \right)} \tag{6}$$

Finally, the thermal resistance was computed using the relation given in Eq. (7).

$$R_{th} = \frac{LMTD}{Q_h} \tag{7}$$

The flow regime of the working fluid through the microchannel heat sink if define by the Reynolds number:

$$\mathrm{Re} = \frac{\rho \dot{v}_m D_h}{\mu} \tag{8}$$

The properties of the working fluid involved in all the calculations, were evaluated based on the bulk temperature, define as:

$$T_b = \frac{T_{in} - T_{out}}{2} \tag{9}$$

### 2.5 Uncertainty analysis

Uncertainty analysis was conducted using the work of Kline and McClintock [CITATION Kli53 \n \t \l 1033 ]. Uncertainties associated with the computed parameters were calculated using Eqs. (10), (11) and (12).

$$\frac{\omega_{Q_c}}{Q_c} = \left[ \left( \frac{\omega_\rho}{\rho} \right)^2 + \left( \frac{\omega_{c_p}}{c_p} \right)^2 + \left( \frac{\omega_v}{v} \right)^2 + \left( \frac{\omega_{(T_{in}-T_{out})}}{(T_{in}-T_{out})} \right)^2 \right]^{1} \tag{10}$$

$$\frac{\omega_h}{h} = \left[ \left( \frac{\omega_{Q_c}}{Q_c} \right)^2 + \left( \frac{\omega_{A_w}}{A_w} \right)^2 + \left( \frac{\omega_{(T_w-T_{in})}}{(T_w-T_{in})} \right)^2 + \left( \frac{\omega_{(T_w-T_{out})}}{(T_w-T_{out})} \right)^2 \right]^{1} \tag{11}$$

$$\frac{\omega_{R_{th}}}{R_{th}} = \left[ \left( \frac{\omega_{Q_h}}{Q_h} \right)^2 + \left( \frac{\omega_{(T_w-T_{in})}}{(T_w-T_{in})} \right)^2 + \left( \frac{\omega_{(T_w-T_{out})}}{(T_w-T_{out})} \right)^2 \right]^{1} \tag{12}$$

Therefore, the uncertainties associated to the evaluated heat transfers parameters are summarized in Tab. 3.

Table 3. Uncertainties associated to the calculated parameters.

| Parameter | Uncertainty |
|---|---|
| Qc | ± 4.2% |
| h | ± 8.9% |
| $R_{th}$ | ± 6.4% |

## 3. RESULTS

The experimental results of the measured properties of viscosity and thermal conductivity of the working fluids and the increases associated to the nanofluids are presented in Fig. 5 and 6, respectively. Thus, as can been seen in Fig 5b. the measured viscosity of base fluid and the nanofluids have not significative differences, once all the increments were into the uncertainty of the measured.

Although, as shown in Fig. 6b, it was obtained gains in the thermal conductivity of the nanofluids with reference on the base fluid. The increases were 4.7% for the sample with the smallest concentration (Φ) of 0.0005% (Ag_80_1), 4.9% for the sample with the concentration of 0.001% (Ag_80_2) and 7.8% for the sample with the bigger concentration of 0.005% (Ag_80_3).

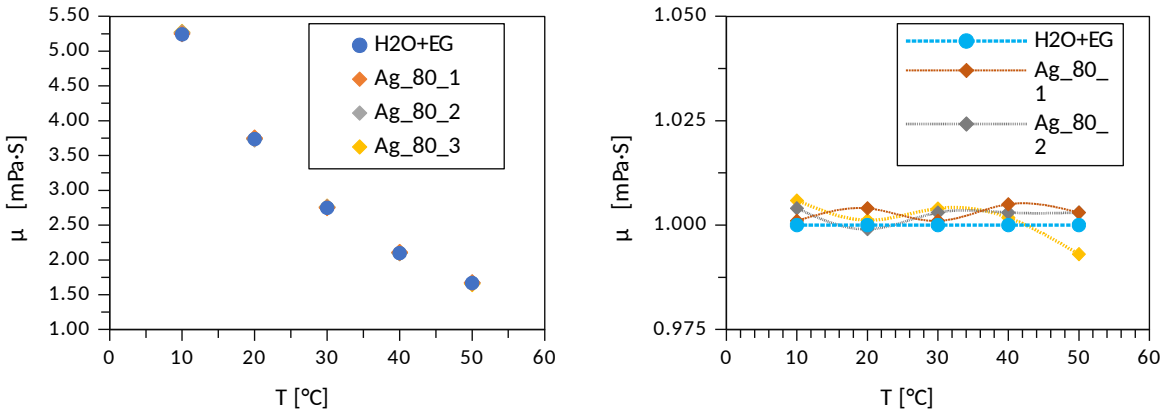


Figure 5. (a) Measure viscosity of the working fluids. (b) Viscosity increases of silver nanofluids.

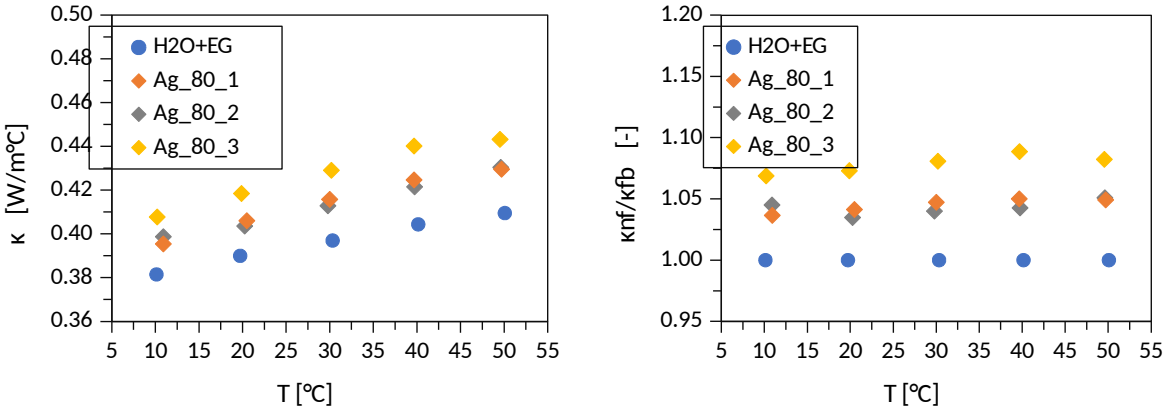


(a) (b)

Figure 6. (a) Measure thermal conductivity of the working fluids. (b) Thermal conductivity increases of silver nanofluids.

The Reynolds number calculated in this work was 180 - 660. For this reason, it can be claim that all the tests performed were in laminar flow regime. Moreover, Fig. 7 and 8 show the comparison of convective heat transfer coefficient *h* of the heatsink at different mass flow rates (G) and the corresponding different volume fractions of nanoparticles for the inlet temperature of 25° C and 35° C, respectively. It is observed that convective heat transfer coefficient increases with the increase of flow rate and increase in the volume concentration of nanoparticles silver.

For the inlet fluid temperature of 25° C (Fig. 7b) the bigger increases in the heat transfer coefficient of the silver nanofluids were obtained to the mass flow rate 28 kg/m$^2$s, corresponding to 6.8%, 12.5% and 44.8% respectively for the samples Ag_80_1, Ag_80_2 and Ag_80_3. However, these increase rates are decreasing with the increase in the mass flow rate. These results are in agreement with the work of Nitiapiruk et al.*[CITATION Nit13 \n \t \l 1046 ]*, where the highest increments in heat transfer coefficient was obtained for the lower Reynolds values (<400).

The mean of the increases in the heat transfer coefficient related to the volume concentration silver nanoparticles was 3.3%, 5.7% and 23.09% respectively. It could be note that the mean of the increases in the heat transfer coefficient to the sample Ag_80_1 and Ag_80_2 are into the uncertainty range calculated for this parameter.

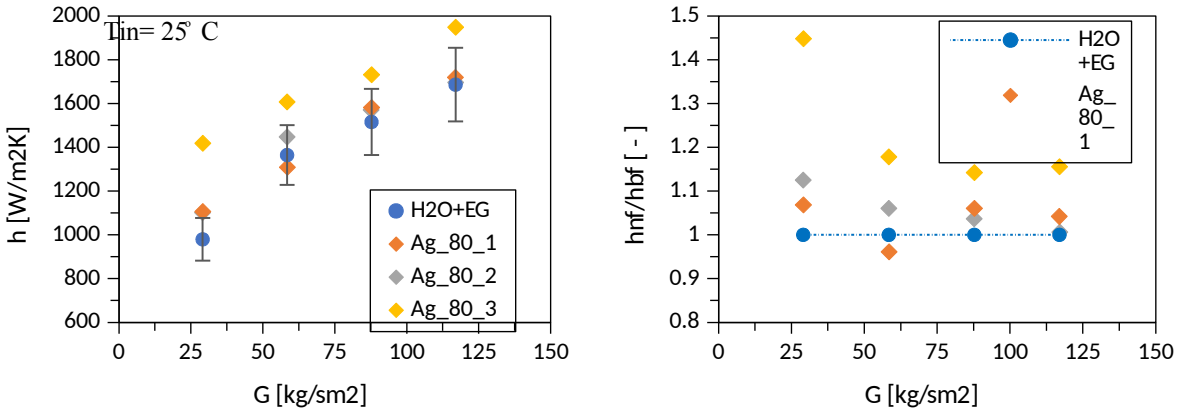


(a) (b)

Figure 7. (a) Calculated heat transfer coefficient of the working fluids for inlet temperature of 25° C. (b) Heat transfer coefficient increases of silver nanofluids.

Different, for the inlet fluid temperature of 35° C (Fig. 8b) it does not appear to exist any significative difference between the increases obtained in the heat transfer coefficient of the nanofluids for different mass flow rates. Thus, the mean of the increments was 2.5%, 2.8% and 20.8% for the samples Ag_80_1, Ag_80_2 and Ag_80_3, respectively. Again, the increases in the heat transfer coefficient to the sample Ag_80_1 and Ag_80_2 are into the uncertainty range calculated for this parameter. Despite this, it is notable that the increases for the inlet temperature of 35° C were lower than the increases for the inlet temperature of 35° C. The total mean of the increases were 2.9%, 3.8% and 21.9% for the samples Ag_80_1, Ag_80_2 and Ag_80_3, respectively.

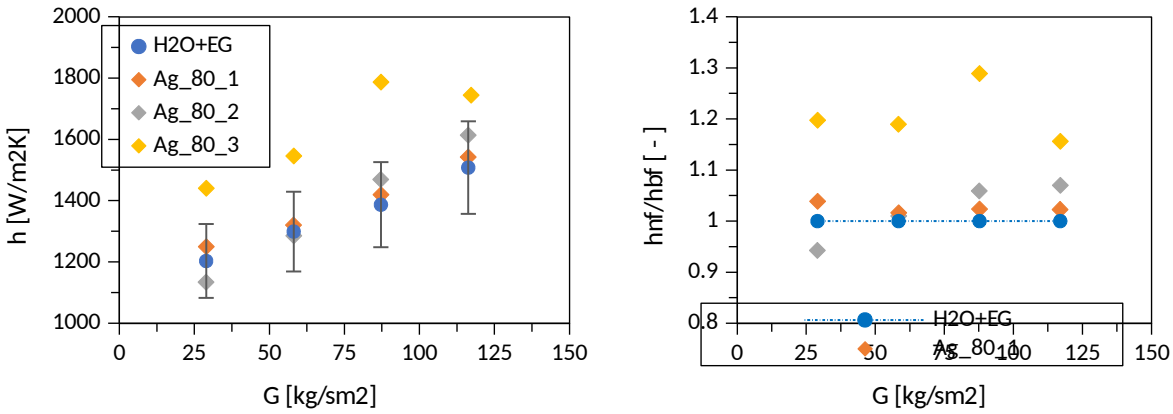


(a) (b)

Figure 8. (a) Calculated heat transfer coefficient of the working fluids for inlet temperature of 35° C. (b) Heat transfer coefficient increases of silver nanofluids.

Figures 9 and 10 present the comparison of thermal resistance of the heatsink at different mass flow rates (G) and the corresponding different volume fractions of nanoparticles for the inlet temperature of 25° C and 35° C, respectively. It is observed that the behavior of the thermal resistance is in agreement with the convective heat transfer coefficient. That is, the increase in the heat transfer coefficient represent a decrease in the thermal resistance. However, the thermal resistance is less sensitive to the parameters that causes these changes. Thus, the maximum decrease of 21.7% in the thermal conductivity was obtained for the sample Ag_80_3, for the mass flow rate of 28 kg/m$^2$s and inlet temperature of 25° C. The mean of the decreases in the thermal resistance of the heat sink related to the volume concentration silver nanoparticles for the inlet temperature of 25° C was 3.5%, 6.9% and 14,8% respectively. Similar, the mean of the decreases in the thermal resistance of the heat sink for the inlet temperature of 35° C was 1.17%, 1.08% and 12,86% for the nanofluid samples Ag_80_1, Ag_80_2 and Ag_80_3, respectively. Finally, the total mean of the decreases were 2.3%, 4.0% and 13.8% for the samples Ag_80_1, Ag_80_2 and Ag_80_3, respectively.

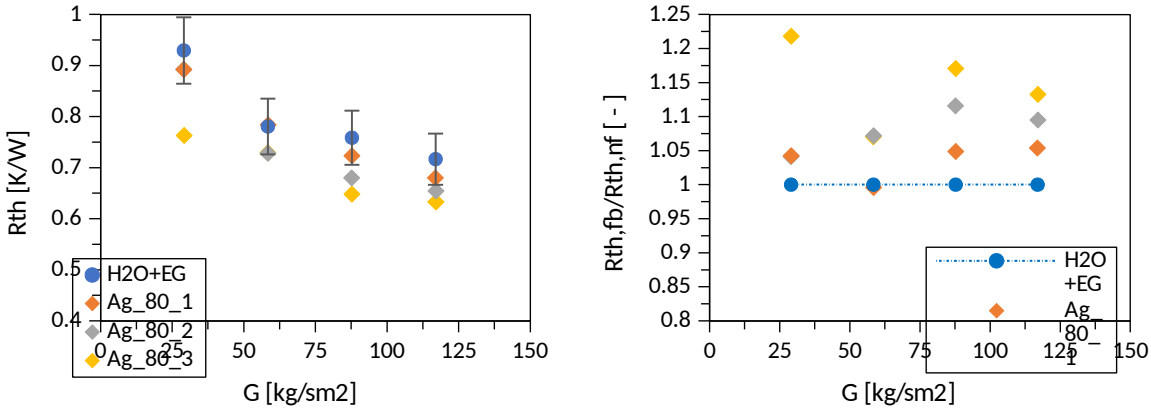


(a) (b)

Figure 9. (a) Calculated thermal resistance of the working fluids for inlet temperature of 25° C. (b) Thermal resistance decreases of silver nanofluids.

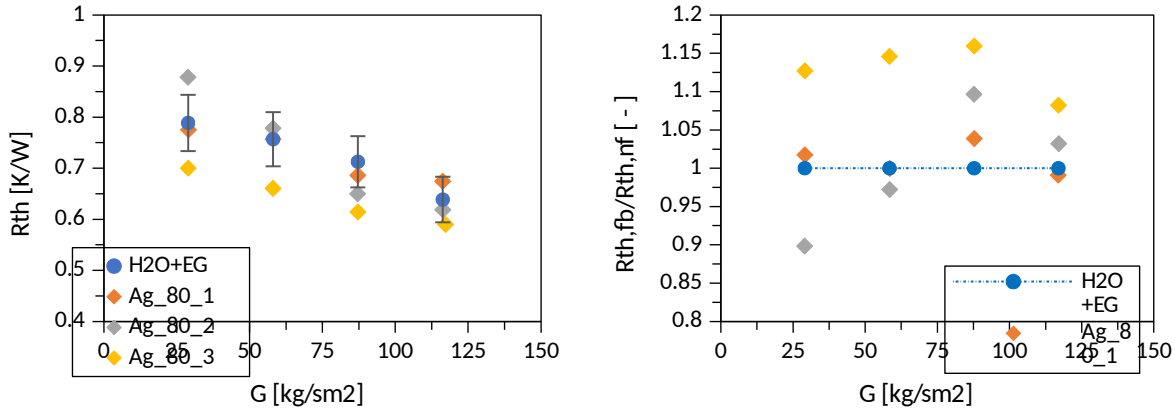


(a) (b)

Figure 10. (a) Calculated thermal resistance of the working fluids for inlet temperature of 35° C. (b) Thermal resistance decreases of silver nanofluids.

## 4. CONCLUSIONS

A thermal performance evaluation of silver nanofluids ($d_{np}$= 80 nm) with three different volume concentrations (0.0005%, 0.001% and 0.005%) in a based fluid composed by 50% of distilled water and 50% of ethylene glycol flowing into a rectangular cross section microchannel heat sink was studied experimentally.

There was not observe any significant increase in the viscosity of the nanofluids when compared to the base fluid. However, it was found that thermal conductivity of the fluid was directly related to the volume concentration of the nanoparticles. The increases of this parameter were 4.7%, 4.9% and 7.8%, respectively from the lower to higher nanofluid concentration.

Nanofluid significantly improved the thermal performance of microchannel heatsink. A maximum enhancement of 44.8%, 12.5% and 6.8% was observed in the convective heat transfer coefficient of the heatsink for the samples Ag_80_1, Ag_80_2 and Ag_80_3, respectively. Similar results were observed in literature, using silver nanofluids in microchannel heat sink. In the work of Şimşek et al. [CITATION Şim18 \n \t \l 1046 ] was obtained a maximum enhancement in the heat transfer coefficient of 56% for nanofluid with volume concentration of 0,00357% at volume flow rate of 180 µl/min. Also, Sarafraz et al. [CITATION Sar18 \n \t \l 1046 ] found a maximum enhancement in the heat transfer coefficient of 47% for nanofluid with volume concentration of 0,1%.

The mean increase in the convective heat transfer coefficient of the microchannel heatsink using silver nanofluids was 2.9%, 3.8% and 21.9% for the samples from the lower to higher nanoparticles concentration.

Furthermore, the mean decrease in the thermal resistance of the microchannel heatsink using silver nanofluids was 2.3%, 4.0% and 13.8% for the samples from the lower to higher nanoparticles concentration

## 5. ACKNOWLEDGEMENTS

The authors gratefully acknowledge the financial support of CAPES, FAPEMIG and CNPq.Futhermore, the autors specially acknowledge to the team work of the Nano and Microfluidics and Microsystems Laboratory (LabMEMS) from UFRJ for the cooperation received.

## 6. REFERENCES

Aberoumand, H., Jafarimoghaddam, A., Javaherdeh, K., Moravej, M., and Aberoumand, S. “Experimental study on the rheological behavior of silver-heat transfer oil nanofluid and suggesting two empirical based correlations for thermal conductivity and viscosity of oil based nanofluids”. *Appl. Therm. Eng.,* vol. 101, pp. 362–372, 2016.

Alfaryjat, A., Mohammed, H., Adam, M., Ariffin, M., & Najafabadi, M. (2014). Influence of geometrical parameters of hexagonal, circular, and rhombus microchannel heat sinks on the thermohydraulic characteristics. *International Communications in Heat and Mass Transfer, 52*, 121-131.

Anbumeenakshi, C., & Thansekhar, M. (2017). On the effectiveness of a nanofluid cooled microchannel heat sink under non-uniform heating condition. *Applied Thermal Engineering, 113*(25), 1437-1443.

Cárdenas Contreras, E.M., Oliveira, G.A., Bandarra Filho, E.P., 2019. "Experimental analysis of the thermohydraulic

performance of graphene and silver nanofluids in automotive cooling systems". *Int. J. Heat Mass Transf.* 132, 375–387. https://doi.org/10.1016/j.ijheatmasstransfer.2018.12.014

Choi, S. U. (1995). Enhancing thermal conductivity of fluids with nanoparticles. *International Mechanical Engineering Congress and Exposition* (pp. 99-105). ASME.

Chu, J., Teng, J., & Greif, A. (2008). Heat transfer for water flow in triangular silicon microchannels. *Journal of Thermal Science and Technology, 3*, 410-420.

Dehghan, M., Valipour, M., & Saedodin, S. (2016). Microchannels enhanced by porous materials: heat transfer enhancement or pressure drop increment? *Energy Conversion and Management, 110*, 22-32.

Gilmore, N., Timchenko, V., & Menictas, C. (2018). Microchannel cooling of concentrator photovoltaics: A review. *Renewable and Sustainable Energy Reviews, 90*, 1041-1059.

Godson, B. Raja, D. Mohan Lal, S. Wongwises. "Convective heat transfer characteristics of silver-water nanofluid under laminar and turbulent flow conditions". *J. Therm. Sci. Eng.* Appl. 4 (2012) 031001.

Kandlikar, S. G., Colin, S., Peles, Y., Garimella, S., Pease, R. F., & Juergen, J. (2013). Heat Transfer in Microchannels—2012 Status and Research Needs. *Journal of Heat Transfer, 135*(9).

Kline, S., & Mcclintock, F. (1953). Describing Uncertainties in Single-Sample Experiments. *Mechanical Engineering, 75*, 3-8.

Nitiapiruk, P., Mahian, O., Dalkilic, A. S., & Wongwises, S. (2013). Performance characteristics of a microchannel heat sink using TiO2/water nanofluid and different thermophysical models. *International Communications in Heat and Mass Transfer, 47*, 98-104.

O'Hanley, H., Buongiorno, J., McKrell, T., & Hu, L.-w. (2012). Measurement and Model Validation of Nanofluid Specific Heat Capacity with Differential Scanning Calorimetry. *Advances in Mechanical Engineering, 2012*, 1- 6.

Pourhoseini, S.H., Naghizadeh, N., Hoseinzadeh, H., 2018. "Effect of silver-water nanofluid on heat transfer performance of a plate heat exchanger: An experimental and theoretical study". *Powder Technol.* 332, 279–286. https://doi.org/10.1016/j.powtec.2018.03.058

Sarafraz, M., Nikkhah, V., Nakhjavani, M., & Arya, A. (2018). Thermal performance of a heat sink microchannel working with biologically produced silver-water nanofluid: Experimental assessment. *Experimental Thermal and Fluid Science, 91*, 509-519.

Şimşek, E., Coskun, S., Okutucu-Özyurt, T., & Unalan, H. E. (2018). Heat transfer enhancement by silver nanowire suspensions in microchannel heat sinks. *International Journal of Thermal Sciences, 123*, 1-13.

Tran, N., Chang, Y.-J., Teng, J.-T., & Greif, R. (2017). A study on five different channel shapes using a novel scheme for meshing and a structure of a multi-nozzle microchannel heat sink. *International Journal of Heat and Mass Transfer, 105*, 429-442.

Tuckerman, D., & Pease, R. (1981). High-performance heat sinking for VLSI. *IEEE Electron Device Letters, 2*, 126-129.

Wang, B. X., Zhou, L. P., Peng, X. F., Du, X. Z., & Yang, Y. P. (2010). On the specific heat capacity of CuO nanofluid. *Advances in Mechanical Engineering, 2010*, 1-4.

## 7. RESPONSIBILITY NOTICE

The authors are the only responsible for the printed material included in this paper.